AMERICAN SOCIETY of
GENE & CELL
THERAPY

Myelolytic Treatments Enhance Oncolytic Herpes Virotherapy in Models of Ewing Sarcoma by Modulating the Immune Microenvironment

Nicholas L. Denton,[1] Chun-Yu Chen,[1] Brian Hutzen,[1] Mark A. Currier,[1] Thomas Scott,[1] Brooke Nartker,[1] Jennifer L. Leddon,[1] Pin-Yi Wang,[1] Rachelle Srinivas,[1] Kevin A. Cassady,[1] William F. Goins,[2] and Timothy P. Cripe[1]

[1]Center for Childhood Cancer and Blood Diseases, Nationwide Children's Hospital, The Ohio State University, Columbus, OH 43205, USA; [2]Department of Microbiology and Molecular Genetics, University of Pittsburgh School of Medicine, Pittsburgh, PA 15219, USA

Ewing sarcoma is a highly aggressive cancer that promotes the infiltration and activation of pro-tumor M2-like macrophages. Oncolytic virotherapy that selectively infects and destroys cancer cells is a promising option for treating Ewing sarcoma. The effect of tumor macrophages on oncolytic virus therapy, however, is variable among solid tumors and is unknown in Ewing sarcoma. We tested the effects of macrophage reduction using liposomal clodronate (Clodrosome) and trabectedin on the antitumor efficacy of intratumoral oncolytic herpes simplex virus, rRp450, in two Ewing sarcoma xenograft models. Both agents enhanced antitumor efficacy without increasing virus replication. The most profound effects were in A673 with only a transient effect on response rates in TC71. Interestingly, A673 was more dependent than TC71 on macrophages for its tumorigenesis. We found Clodrosome and virus together induced expression of antitumorigenic genes and reduced expression of protumorigenic genes in both the tumor-associated macrophages and the overall tumor stroma. Trabectedin reduced intratumoral natural killer (NK) cells, myeloid-derived suppressor cells, and M2-like macrophages, and prevented their increase following virotherapy. Our data suggest that a combination of trabectedin and oncolytic herpes virotherapy warrants testing in the clinical setting.

INTRODUCTION

Ewing sarcoma is an aggressive bone or soft tissue tumor predominantly found in adolescents and young adults. Despite the aggressive use of surgical resection, irradiation, and chemotherapy, outcomes are unacceptable with 5-year survival rates for patients with localized and metastatic disease less than 70% and 30%, respectively.[1,2] The characteristic translocation between chromosomes 11 and 22, resulting in the EWS/FLI fusion protein, or similar translocations between EWS and other members of the ETS family of transcription factors, are pathognomonic oncogenes that aberrantly regulate gene expression.[3,4] Among their pleiotropic effects is enhanced macrophage chemokine expression promoting pro-tumor M2-like macrophage activation.[5,6] In fact, in a small pilot study, the 5-year overall survival rate dropped from 70% to 20% in patients with localized disease who had greater than 30 CD68^{+} macrophages per 0.64 mm[2] high-power

field in their tumor biopsies.[1] Thus, tumor-associated macrophages may be an attractive therapeutic target.

Another promising strategy to treat aggressive cancer is the emerging field of oncolytic viruses that selectively replicate in and destroy cancer cells. Oncolytic virotherapy is characterized by direct infection of cancer cells and stimulation of a host antitumor immune response.[5,7,8] There is a growing number of clinical trials for oncolytic virus therapy that demonstrate safety in adult and childhood cancer patients, leading to the first Food and Drug Administration-approved oncolytic virus, Talimogene laherparepvec (T-VEC), for the treatment of metastatic melanoma.[9–11] With these recent breakthroughs, oncolytic virotherapy has the potential to become a new therapy option for a wider variety of patients with solid tumors.

Interestingly, macrophages have variable effects on oncolytic virotherapy, although their interactions in Ewing sarcoma have not been investigated. Although M2-like tumor macrophages are generally tumor promoting by suppressing the host antitumor immune response, they also suppress the host antiviral immune response that inhibits the direct oncolytic effect of virotherapy.[5,12–14] M1-like tumor macrophages are generally tumor suppressive by activating the host antitumor immune response; however, they can also enhance the antiviral immune response and inhibit the oncolytic effect of virotherapy.[5,15,16] Within the categories of classically activated inflammatory M1 macrophage and alternatively activated immune suppressive M2 macrophage there are non-canonical subtypes of M1-like and M2-like macrophages that utilize different mechanisms of immune stimulation and suppression, depending on how the microenvironment stimulates the macrophages.[17,18] These non-canonical activation states include the M1-like M(lipopolysaccharide [LPS]), M(interferon-gamma [IFNγ]), and M(LPS+IFNγ), along with the M2-like M(IL-10), M(IL-4), M(transforming growth
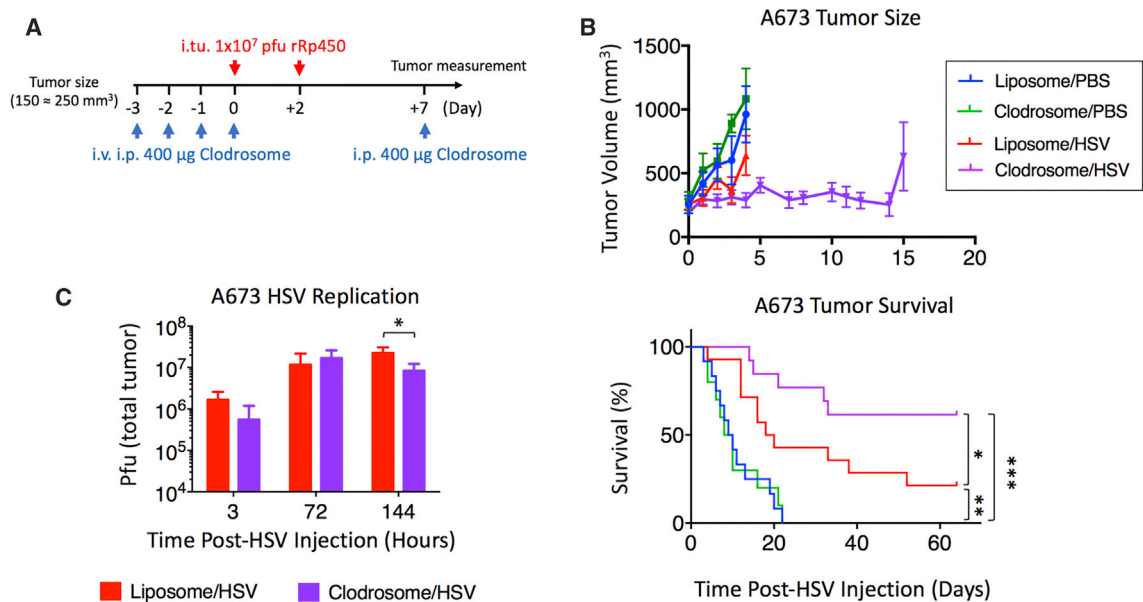

Figure 1. Clodrosome Depletion of Macrophages Enhances OV Efficacy

(A) Treatment regimen of A673 tumor xenograft-bearing mice given 400 μg of liposome or Clodrosome intravenously (i.v.) on day −3 and intraperitoneally (i.p.) on days −2, −1, and 0 followed by weekly i.p. treatments. Oncolytic herpes simplex virus rRp450 was given at 10^7 pfu intratumorally (i.tu.) on days 0 and 2. (B) A673 flank tumors treated with the above regimen were measured until tumors reached an endpoint volume of 2,000 mm³. Both tumor growth curves with SEMs and Kaplan-Meier plots of survival are shown. Error bars indicate SEM. (C) Virus replication in A673 xenografts treated with the above Clodrosome regimen and a single 10^7 pfu dose of rRp450 given intratumorally (i.t.) at the time points indicated prior to tumor homogenization and plaque assay. Statistical analyses of survival curves were performed using Mantel-Cox test, and bar graphs were done using unpaired multiple two-tailed t test; *p < 0.05, **p < 0.005, ***p < 0.0005. Error bars indicate SD.

factor-β [TGF-β]), and M(immune complex).[19–21] Therefore, a thorough analysis of the interactions between tumor cells, macrophages, and oncolytic viruses is required to understand how tumor macrophages affect oncolytic virus efficacy.

We previously showed that direct injection of oncolytic herpes virus into models of Ewing sarcoma is only partially effective at slowing tumor growth, in part due to unknown effects of infiltrating CD11b⁺ myeloid cells.[22] To determine whether the effect was due to macrophages, here we used two macrophage-reducing strategies, including the well-known agent liposomal clodronate (Clodrosome), which poisons mitochondrial electron transport and, due to its liposomal formulation, is selectively taken up by phagocytic cells, and trabectedin, which has also been shown to reduce tumor-associated macrophages. In combination with virotherapy, these agents markedly increased antitumor efficacy and were associated with a significantly altered tumor microenvironment. The combination induced expression of antitumorigenic genes and reduced expression of protumorigenic genes in both the tumor-associated macrophages and the overall tumor stroma. Trabectedin reduced intratumoral natural killer (NK) cells, myeloid-derived suppressor cells (MDSCs), and M2-like macrophages, and prevented their increase following virotherapy. Our data provide rationale for clinical trials of oncolytic virotherapy with macrophage-targeted therapy.

RESULTS

Clodrosome Depletion of Macrophages Enhances Oncolytic Virus Efficacy

In order to determine the effect of tumor macrophages on oncolytic virus efficacy in a model of Ewing sarcoma, we used a regimen of macrophage-depleting liposomal clodronate (Clodrosome) prior to oncolytic herpes simplex virus infection. We treated athymic nude mice previously implanted with A673 xenograft tumors with a combination of intravenous and intraperitoneal Clodrosome or liposome control prior to two intratumoral doses of rRp450, a herpes simplex type 1 virus attenuated by deletion of the virus gene encoding the large subunit of ribonucleotide reductase,[23,24] or PBS control (Figure 1A). Clodrosome treatment alone did not impact established A673 xenograft growth, while macrophage-intact liposome-treated xenografts experienced a tumor growth delay with a few complete responses (CRs) (3/14 CR) following rRp450 injection (Figure 1B). When we depleted macrophages with Clodrosome prior to rRp450 injection, however, we found that the majority of A673 xenografts shrank to CR (8/14 CR). Although we hypothesized that the improved antitumor efficacy of oncolytic virus with macrophage depletion was likely due to increased virus production and/or spread, given that macrophages are known to phagocytose virus-infected cells,[14,25] we did not observe a significant impact of macrophage depletion on rRp450 replication kinetics in A673 xenografts except after 144 hr, at which time the amount of virus recovered from tumors was even
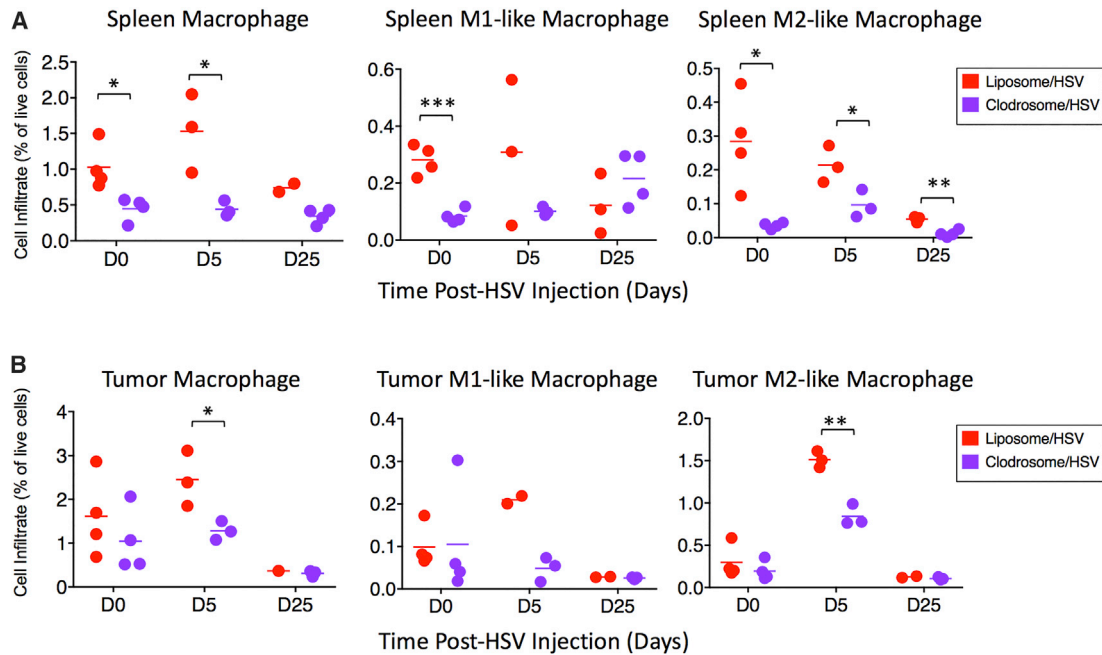
Figure 2. Clodrosome Reduces Systemic and Intratumoral Macrophages

(A and B) Flow cytometry quantification of total splenocytic (A) and tumor (B) macrophage infiltration and macrophage M1-like and M2-like phenotype infiltration in A673 xenografts on days 0, 5, and 25 in the single intratumorally (i.tu) rRp450 treatment regimen done in Figure 1C. Statistical analysis of bar graphs was done using unpaired multiple two-tailed t test; *p < 0.05, **p < 0.005, ***p < 0.0005.

less in the Clodrosome group (Figure 1C). These data suggest that tumor macrophages diminish the effects of virotherapy through mechanisms other than inhibiting oncolysis.

We sought to determine the effects of Clodrosome on systemic (splenic) and tumor macrophages, specifically M1-like versus M2-like macrophage populations. We used flow cytometry to analyze leukocyte populations (see gating strategy in Figure S1) in mouse spleens and rRp450-infected A673 tumors, and found that Clodrosome induced significant depletion of both M1-like (CD11c$^+$/CD206$^-$) and M2-like (CD11c$^+$/CD206$^+$) splenic macrophages (Figure 2A). Interestingly, the tumor macrophages were only partially depleted ($\sim$50%; Figure 2B). Because M2-like tumor macrophages were approximately 10-fold higher in abundance compared with M1-like tumor macrophages, we postulated that the M2-like tumor macrophages are responsible for limiting the efficacy of oncolytic virus therapy in A673 tumors.

Clodrosome Depletion of Macrophages Prevents A673 Tumorigenesis

Given the importance of macrophages in restricting response to virotherapy in A673, we sought to determine their importance in tumorigenesis of this model. We pretreated athymic nude mice with a similar regimen of intravenous and intraperitoneal Clodrosome prior to subcutaneous implantation of Ewing sarcoma cells into the flank (Figure 3A). The macrophage intact mice treated with liposome control quickly formed tumors that reached endpoint criteria within

20 days (Figure 3B). However, the mice we pre-treated with Clodrosome experienced a significant delay in tumor formation, with 50% failing to establish a tumor until >60 days after A673 cell implantation. We again noted that Clodrosome reduced splenic macrophages and had some impact on NK cell and MDSC populations as well (Figure 3C). Interestingly, the few tumors that formed 10 days after A673 implantation in the Clodrosome-treated mice acquired tumor macrophages comparable with the liposome control-treated tumors (Figure 3D); this finding may be due to variability in Clodrosome stability or the ability of residual macrophages in the flank to assist in tumor formation. These results suggest that tumor macrophages are required for Ewing sarcoma tumorigenesis in this model.

M2-like Macrophages Interfere with Virus Cytotoxicity

The similar recovery of infectious virus from tumors suggested that macrophages do not affect virus-mediated oncolysis in the A673 model. To confirm this finding, we assessed whether macrophages in isolation could limit the effects of virus-mediated oncolysis by evaluating oncolytic virus cytotoxicity in Ewing sarcoma cells cultured with bone marrow-derived macrophages (BMDMs) stimulated under various conditions. We isolated murine BMDMs and stimulated them under conditions expected to polarize macrophages toward an M2-like phenotype (IFNγ, LPS, and IFN+LPS), toward an M1-like phenotype (interleukin-10 [IL-10], IL-4, TGF-β), or left them unstimulated to serve as a baseline control. To determine the effects the different conditions had on gene expression patterns, we created a 96-gene PCR array including known macrophage and
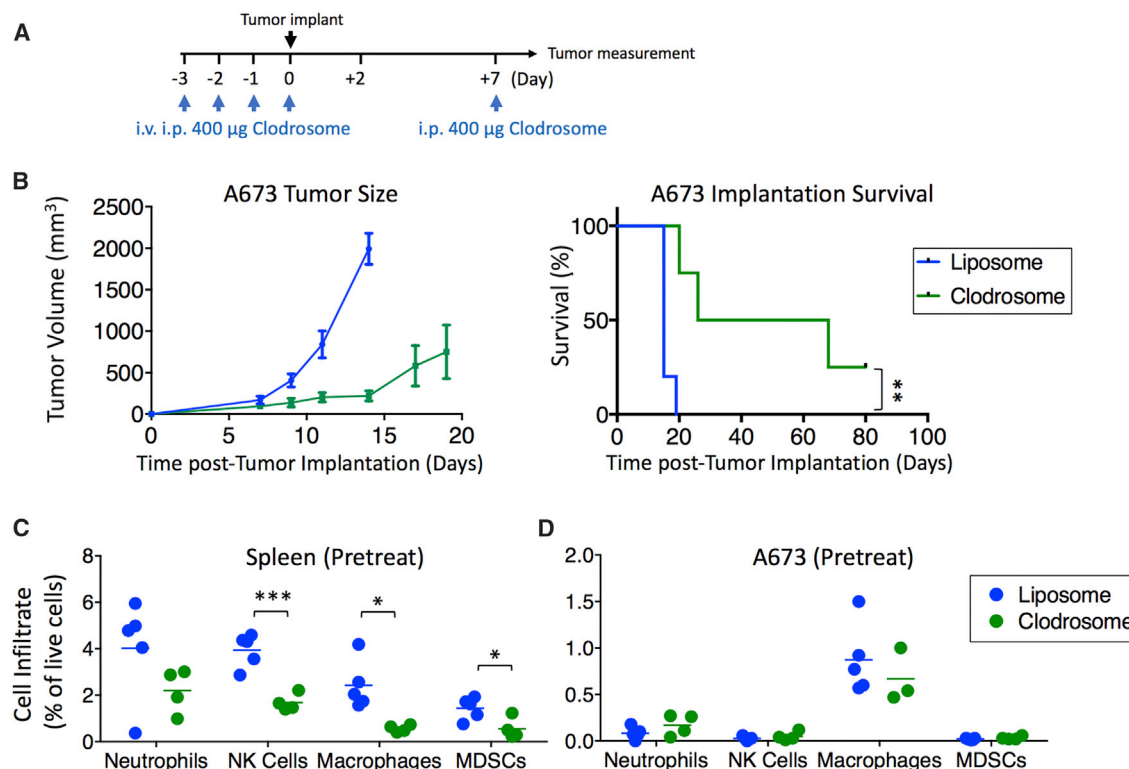
Figure 3. Clodrosome Depletion of Macrophages Impairs A673 Tumorigenesis

(A) Treatment regimen of athymic nude mice given 400 μg of liposome or Clodrosome intravenously (i.v.) on day −3 and intraperitoneally (i.p.) on days −2, −1, and 0 followed by weekly i.p. treatments. A673 Ewing sarcoma cells were implanted subcutaneously into the flank on day 0. (B) A673 flank tumors treated with the above regimen were measured until tumors reached an endpoint volume of 2,000 mm^3. Flow cytometry quantification of (C) splenocytic and (D) tumor leukocyte infiltrates in A673 tumors 10 days after A673 cell implantation. Statistical analyses of survival curves were done using Mantel-Cox test, and bar graphs were performed using unpaired multiple two-tailed t test; *p < 0.05, **p < 0.005, ***p < 0.0005. Error bars indicate SD.

cancer-relevant murine genes. After normalizing gene expression to the internal actin control, we performed an unsupervised clustering of genes that showed significant changes across the different conditions (Figure 4A). The results showed a cluster of genes that were mostly activated following exposure to the LPS and/or IFNγ stimuli (top of Figure 4A), genes that were indiscriminately expressed regardless of stimulation (middle of Figure 4A), and genes preferentially activated following exposure to IL-4, IL-10, or TGF-β (bottom of Figure 4A). We then directly cocultured these differently stimulated macrophages with A673 cells prior to rRp450 virus infection and semi-daily cytokine supplementation, and measured cell viability relative to uninfected, unstimulated cocultures (Figure 4B). Interestingly, we found that IFNγ and TGF-β alone resulted in some degree of cytotoxicity (compare uninfected black bars in Figure 4B). In addition, we found that unstimulated macrophages as well as macrophages stimulated with IFNγ (alone or, to a lesser degree, with LPS) or with IL-4 caused further cytotoxicity, suggesting that these cells are capable of recognizing and phagocytosing stressed cancer cells. These data suggest that different macrophage phenotypes may differ in their anti-cancer activity. Interestingly, while virus infection reduced cell viability in all cases compared

with uninfected cells in the absence of macrophages (black bars in oncolytic herpes simplex virus [oHSV] groups; Figure 4B), the addition of co-cultured cells did not affect virus-mediated cell killing in any of the conditions. This finding is consistent with our *in vivo* data suggesting that macrophage reduction via Clodrosome did not change virus-mediated oncolysis.

Clodrosome and Virotherapy Independently Modulate Tumor Macrophages and the Stromal Microenvironment

Because Clodrosome only partially reduced the numbers of intratumoral macrophages, we sought to determine any changes in the phenotype of residual tumor-associated macrophages in the different treatment groups. To do so, we isolated F4/80+ cells from harvested tumors by magnetic bead selection and analyzed the same genes from our *in vitro* study using the qPCR gene array and normalized gene expression to the actin control. We were unable to match the cell populations from any of the groups with any of the patterns of expression we found in our prior *in vitro* study using cytokine-stimulated bone marrow-derived macrophages, suggesting (not surprisingly) that tumor-associated macrophages are comprised of a mixed population of different phenotypes. Instead, we sought to
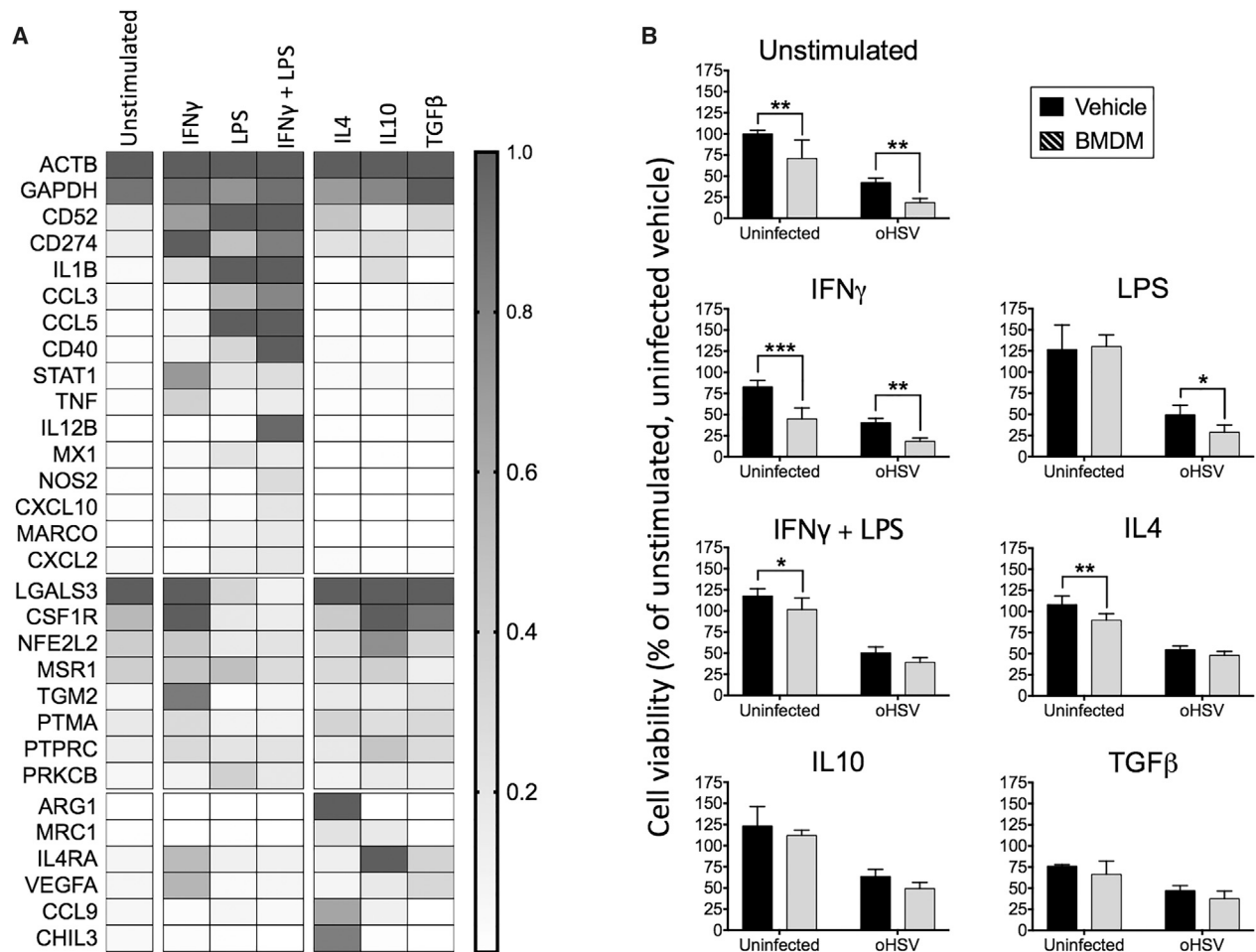
A

B

Figure 4. Bone Marrow-Derived Macrophages Alter Phenotypes in Response to Exogenous Stimuli But Do Not Affect Viral Oncolysis

(A) F4/80$^+$ bone marrow-derived macrophages were isolated and grown in 10F DMEM unstimulated or stimulated with LPS, IFNγ, LPS+IFNγ, IL-4, IL-10, or TGF-β and analyzed for gene expression. (B) A673 Ewing sarcoma cells were cultured alone or cocultured with the different macrophage populations and infected with rRp450 for 6 days before performing MTS viability assays. Statistical analysis of viability curves was performed using ANOVA; *p < 0.05, **p < 0.005, ***p < 0.0005. Error bars indicate SD.

determine changes in gene expression in the combination group (Clodrosome+oHSV), in which we saw significant antitumor activity, compared with the other groups. We normalized the expression of each gene to the control group (liposome/PBS) and sorted their expression from high to low in the combination group. As shown in Figure 5, 15/26 genes associated with known anti-tumorigenic activity increased, 5/26 remained unchanged, and 6/26 decreased in the combination group. Conversely, in 10/23 pro-tumorigenic activity increased, 3/23 remained unchanged, and 10/23 decreased in the combination group. Interestingly, most of the changes in gene expression were not shared in either of the single-agent treatment groups, suggesting that both Clodrosome and virus acted in concert to alter macrophage phenotypes. We also found expression of virus genes in virus-treated tumors, suggesting that macrophages are either directly infected or phagocytose virus-infected cells following intratumoral virus injection.

The use of human tumor xenograft models in mice enables us to assess changes in gene expression specifically in the microenvironment, distinct from cancer cells, by measuring changes in mouse genes. In addition to analyzing isolated tumor-associated macrophages, we also analyzed the entire tumor microenvironment using the qPCR microarray in a separate cohort of tumors. Similar to our findings in macrophages, the tumor microenvironment in the combination group was highly inflamed, with marked activation of anti-tumorigenic genes and suppression of pro-tumorigenic genes (Figure 6). These changes mirrored but were even more dramatic in numbers of genes and fold changed than those in the F4/80$^+$ macrophages. In the microenvironment as a whole, 17/26 genes associated with known anti-tumorigenic activity increased, 7/26 remained unchanged, and 2/26 decreased in the combination group. Conversely, 6/23 pro-tumorigenic activity increased, 8/23 remained unchanged, and 9/23 decreased in the
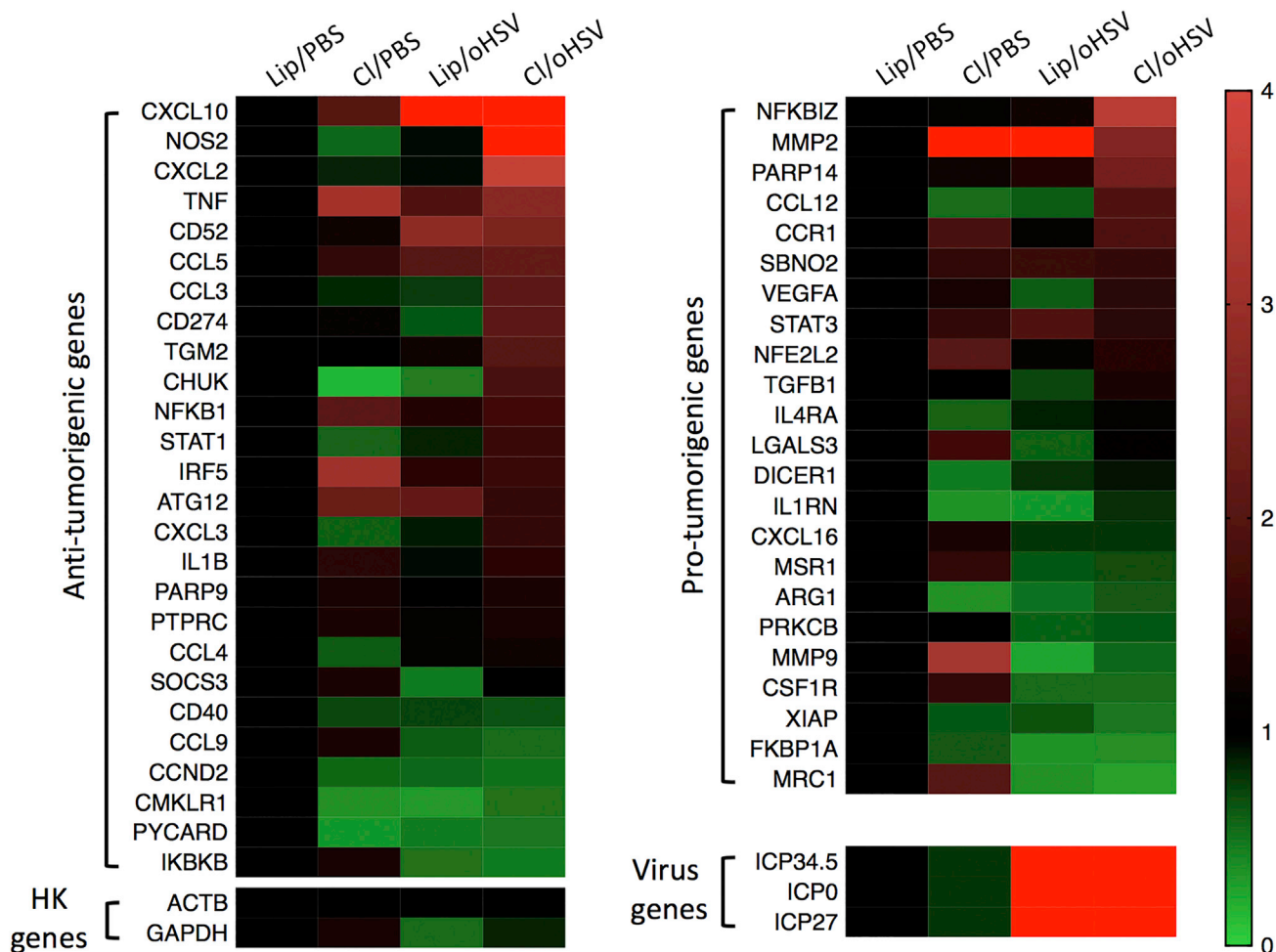
Figure 5. Clodrosome Plus Virus Alter the Phenotypes of Tumor-Associated Macrophages

qPCR array of macrophage activity in F4/80+ tumor macrophages isolated from A673 xenografts treated under the regimen in Figure 1A at 5 days after the first rRp450 infection. Gene expression was normalized within each sample to actin; then the expression of each gene was normalized to that gene's expression in the control liposome/PBS group. Genes were sorted based on their expression in the combination Clodrosome/oHSV group.

combination group. Again, many of the changes were not reflected in either of the single-treatment groups. Our findings suggest that reduction of macrophages by Clodrosome enabled cells in the microenvironment to react to virus infection more profoundly, either directly or indirectly.

We noted that one of the genes decreased by Clodrosome in the microenvironment was TGF-β. We previously reported TGF-β signaling inhibited oncolytic virus efficacy in immunocompetent rhabdomyosarcoma models.[26] Therefore, we also inhibited A673 TGF-β receptor family signaling using the small molecular inhibitor, A8301, as we had in that study, in combination with oncolytic virus infection. In contrast with our findings in the immunocompetent sarcoma model, in this T cell-deficient setting we did not observe a significant change in tumor response to oncolytic virus therapy (Figure S2).

Trabectedin-Mediated Macrophage Modulation Enhances rRp450 Efficacy

Although Clodrosome is a useful tool for depleting macrophages in animal models, we sought a clinically relevant approach that might be useful in combination with virotherapy. Trabectedin is a chemotherapeutic that has been previously shown to deplete tumor macrophages.[27] While trabectedin is currently FDA approved for liposarcoma, there is a growing body of preclinical research demonstrating therapeutic efficacy in Ewing sarcoma,[28–31] thought to be due to the interruption of the transcriptional activation by EWS-FLI1. For these reasons we sought to test the combination of trabectedin and oncolytic virus therapy against Ewing sarcoma.

We administered A673 xenograft-bearing athymic nude mice with two doses of intravenous trabectedin on days 0 and 7, along with
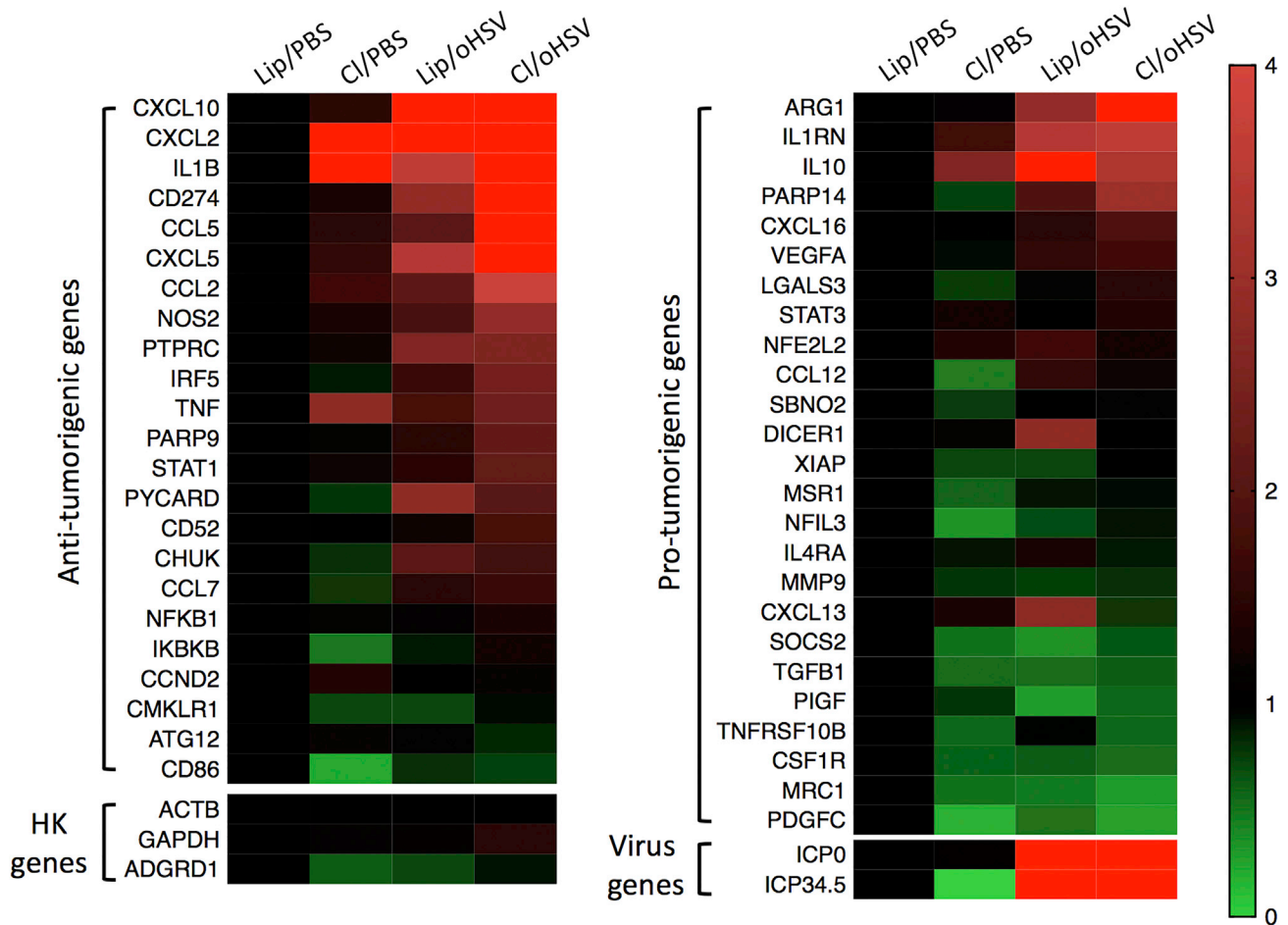
Figure 6. Clodrosome Plus Virus Alter the Tumor Stromal Microenvironment

qPCR array with mouse-specific primers of whole A673 tumor powder treated under the regimen in Figure 1A at 5 days after first rRp450 infection. Gene expression was analyzed as in the legend of Figure 5.

two doses of intratumoral rRp450 on days 0 and 2 (Figure 7A). Similar to Clodrosome and consistent with prior reports, we found trabectedin reduced tumor-associated macrophages (Figure 7B). Interestingly, trabectedin primarily reduced M2-like macrophages, but not M1-like macrophages, whereas Clodrosome reduced both. We also noted that trabectedin reduced NK cells and MDSCs. While trabectedin alone had no effect on established A673 tumor growth, the combination of trabectedin with rRp450 significantly improved mouse survival compared with oncolytic virus therapy alone (Figure 7C). As with Clodrosome, the effect did not appear to be due to differences in virus-mediated oncolysis because we did not observe any differences in live virus recovered from tumors (Figure 7D).

Finally, we sought to test our findings in a second model of Ewing sarcoma to determine the generalizability of our findings. We found the TC71 model to be less dependent on macrophages for growth, as evidenced by the lack of a statistical difference in the delay of the

appearance and growth rate of tumors in the pre-implantation Clodrosome treatment (Figure 8A), in contrast with A673. Similarly, although there was a trend toward improved virotherapy efficacy when combined with Clodrosome, the differences in tumor growth rates and animal survival also did not reach statistical significance (Figure 8B). Regarding therapeutic efficacy, virotherapy alone had a more profound effect on slowing tumor growth in TC71 (Figure 8C) than in A673, and although the addition of trabectedin resulted in more initial responses than virotherapy alone (5/12 [42%] CRs and 5/12 [42%] partial responses in the combination for a total of 84% response rate, compared with 2/8 [25%] CRs and 1/8 [12.5%] partial responses for a total of 37.5% response rate), there was no difference in overall animal survival. These data are all consistent with the idea that tumor models dependent on macrophages for progression may be less responsive to virotherapy but can be rendered more susceptible by modulating the tumor-associated macrophages and the immune microenvironment with Clodrosome or trabectedin.
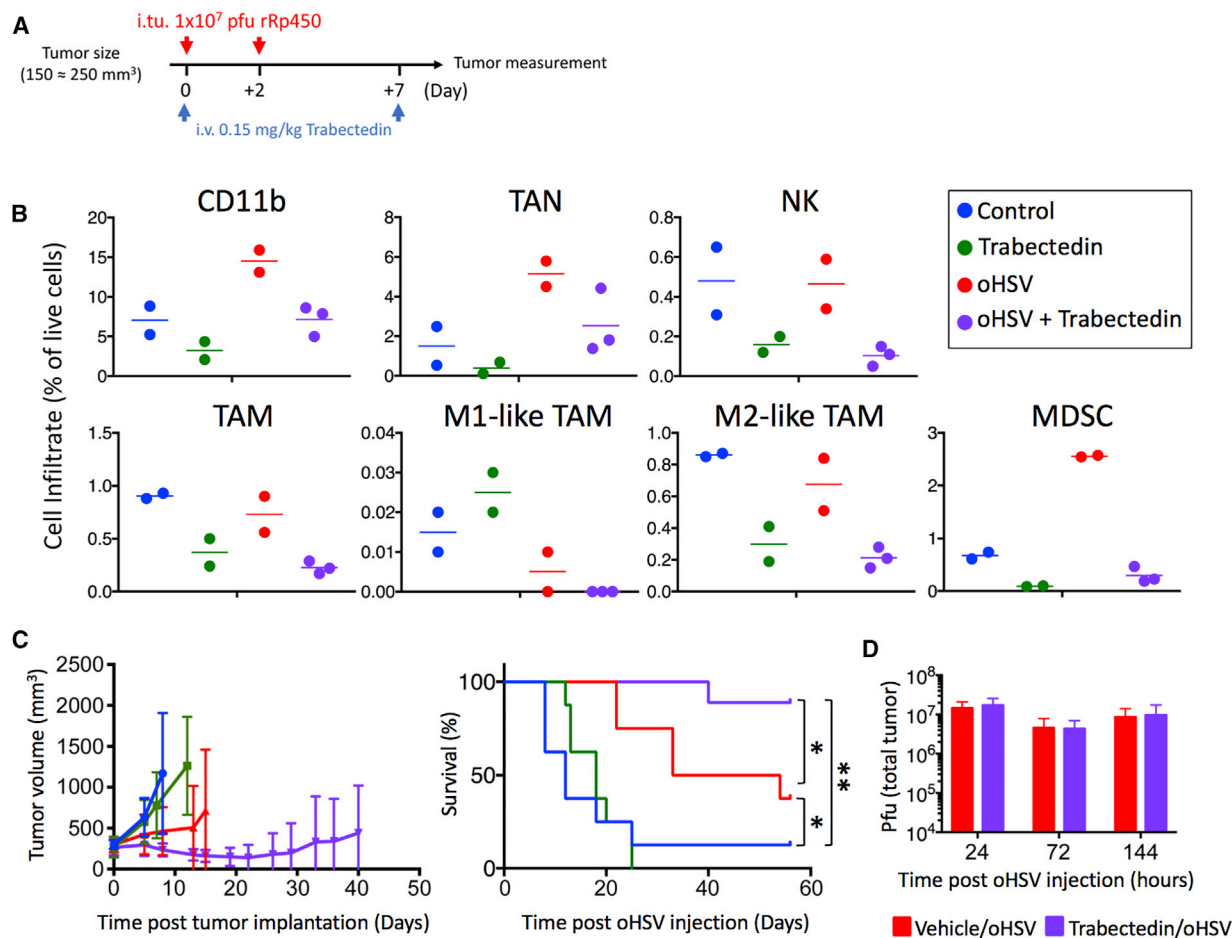
Figure 7. Trabectedin Enhances Oncolytic Herpes Virus Efficacy

(A) Treatment regimen of A673 tumor xenograft-bearing mice given 0.15 mg/kg trabectedin intravenously (i.v.) on days 0 and 7. Oncolytic herpes simplex virus rRp450 was given at 10^7 pfu intratumorally (i.tu.) on days 0 and 2. (B) Flow cytometry quantification of tumor leukocyte infiltrates in A673 tumors on day 3. (C) A673 flank tumors treated with the above regimen were measured until tumors reached an endpoint volume of 2,000 mm³. Statistical analyses of survival curves were performed using the Mantel-Cox test, and bar graphs were done using unpaired multiple two-tailed t test; *p < 0.05, **p < 0.005. (D) Virus replication in A673 xenografts treated with or without trabectedin and a single 10^7 pfu dose of rRp450 given i.t. at the time points indicated prior to tumor homogenization and plaque assay. Error bars indicate SD.

DISCUSSION

Here we report that xenograft models of Ewing sarcoma are variably dependent on macrophages for tumorigenesis, and systemic strategies to diminish macrophages enhance the antitumor response to oncolytic herpes virotherapy without changes in the kinetics of virus replication. Instead, we found that the combination of Clodrosome or trabectedin with virotherapy markedly altered the phenotype of tumor-associated macrophages and the tumor stroma toward a more inflammatory state, as well as altered the cellular immune microenvironment.

Our data suggest that a deeper understanding of the biology of tumor-associated macrophages in the context of oncolytic virotherapy is warranted. While the importance of non-canonical macrophage activity has been recognized in the field of trauma and wound heal-

ing research, there have been few studies of the impact of non-canonical macrophages on tumor progression and immunotherapy.[19,21,32] Although IL-12 expressing oHSV has been shown to induce phosphorylated signal transducer and activator of transcription 1 (p-STAT1)[+]/inducible nitric oxide synthase (iNOS)[+] M1-like macrophage polarization, the additional inhibition of immune checkpoint signaling was required to improve oncolytic virus (OV) antitumor efficacy in glioblastoma models.[33] M1-like p-STAT1/3[+] tumor-associated macrophages (TAMs) have also been shown to inhibit oHSV replication in infected macrophages, suggesting that viral genes found in infected A673 macrophages are not likely replicating virus.[34] There is also evidence that individual macrophages can be simultaneously stimulated into M1-like and M2-like activity during wound healing.[19,20] Even though transcriptional analysis of individual macrophages was outside the scope of
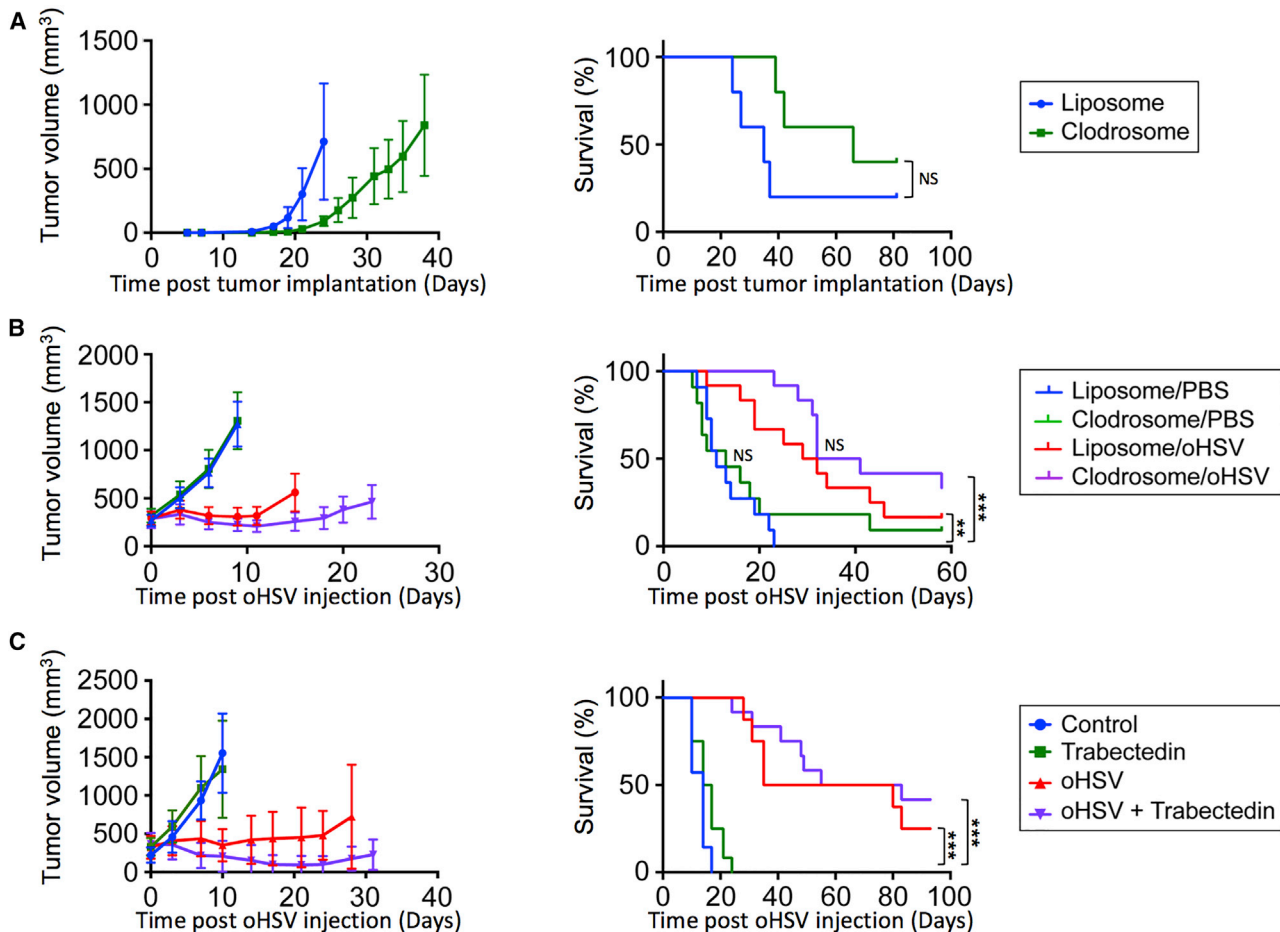
Figure 8. The Ewing Sarcoma Model TC71 Is Less Dependent on Macrophages and More Susceptible to Oncolytic Virotherapy

(A) Animals were pretreated with Clodrosome or its control liposome using the regimen in Figure 3A and monitored for tumor development and growth. $^{NS}p = 0.1359$. (B) TC71 tumor-bearing animals were treated as in Figure 1A and followed for tumor growth and animal survival. $p = 0.2$ for Lip/PBS compared with Clod/PBS; $p = 0.07$ for Lip/PBS compared with Lip/oHSV. (C) TC71 tumor-bearing animals were treated as in Figure 7A and followed for tumor growth and animal survival. NS, not significant. $^{**}p < 0.005$, $^{***}p < 0.0005$. Error bars indicate SD.

this project, it would be interesting to determine whether individual tumor macrophages can act simultaneously as M1-like and M2-like macrophages.

Our findings also strongly support the combination therapy of oncolytic herpes simplex virus and trabectedin to improve Ewing sarcoma treatment. Trabectedin is a DNA intercalation chemotherapeutic that is particularly attractive for Ewing sarcoma because it disrupts EWS/FLI1 transcription; in some models, such activity results in single-agent activity,[28–31] although we did not observe any efficacy of trabectedin alone in A673 or TC71 despite administering doses previously shown to reduce EWS/FLI1 expression. In addition to inhibiting EWS/FLI-mediated tumor progression, trabectedin also depletes TRAILR2$^+$ tumor leukocytes, such as macrophages and MDSCs.[27,35,36] Interestingly, in addition to effects on these cell populations, we also observed trabectedin-mediated depletion of NK cells that has not been previously reported. Although trabectedin as a

monotherapy was insufficient in reducing A673 tumor xenograft growth, it enhanced oncolytic herpes simplex virus antitumor efficacy similar to the effects we observed with Clodrosome. The additional depletion of MDSCs is also likely to play a role, considering that MDSCs tend to differentiate into pro-tumorigenic M2-like macrophages.[37–39]

One of the limitations in Ewing sarcoma research is the lack of immunocompetent animal models. Despite extensive study of the translocation resulting in the EWS/FLI protein, the cell of origin for Ewing sarcoma remains elusive.[40,41] Although this knowledge gap limits study of *in vivo* T cell interaction in animal models of Ewing sarcoma, it is known that M1-like and M2-like tumor macrophages strongly influence the activation of CD8$^+$ and regulatory T cells, respectively.[42–44] Therefore, we postulate that the phenotypic changes in gene expression we measured in tumor macrophages and the immune microenvironment will increase CD8$^+$ T cell activation in immunocompetent

Ewing sarcoma patients and further enhance the virus-induced antitumor immune response we observed in the athymic nude mouse model. However, it must also be noted that both trabectedin and oncolytic virus therapy can increase immune checkpoint inhibition signaling, which may inhibit T cell activation against tumor antigens.[35,45–49] It would be interesting to determine the efficacy of immune checkpoint inhibition in combination with trabectedin and oncolytic virus therapy in immunocompetent pediatric sarcoma models.

Overall, our data suggest that the presence of immunosuppressive tumor macrophages in Ewing sarcoma may be a potential biomarker for patients who would benefit from a combination of trabectedin and oncolytic virus therapy. Trabectedin and oncolytic herpes simplex virus combination therapy greatly increased survival of mice implanted with Ewing sarcoma xenografts that exhibited a strong macrophage dependence. Our data support examining a larger panel of pediatric sarcomas to validate macrophage effects on oncolytic virus antitumor efficacy and determine the probable success of a clinical trial combining trabectedin and oncolytic virus therapy in pediatric sarcoma patients.

MATERIALS AND METHODS

Experimental Design
The objectives of this study were to determine the effect of macrophages on oncolytic virus antitumor efficacy in Ewing sarcoma xenografts and design a combination therapy to enhance therapeutic outcome in Ewing sarcomas that exhibit macrophage-dependent inhibition of oncolytic virus therapy. We pursued these objectives by treating athymic nude mice bearing Ewing sarcoma xenografts with oncolytic virus and macrophage-depleting drugs, and recording tumor progression (n = 12–14, endpoint at tumor volume >2,000 mm^3 or day >60), leukocyte infiltration (n = 2–5), and virus replication (n = 4–6). We determined the effect of macrophage activity on oncolytic virus antitumor efficacy by coculturing oncolytic virus-treated Ewing sarcoma cells with bone marrow-derived macrophages (n = 6) and then performing qPCR array analysis of whole tumor and F4/80$^+$ macrophage activation, viral infection, and antitumor gene expression (n = 3–6). Treatment group was assigned through simple randomization of each mouse bearing a xenograft ranging from 150 to 250 mm^3. Flow cytometry analyses were blinded to treatment group. Outliers were defined as having a value greater than 3 SDs from the mean. Each graph is the accumulation of two to three experimental replicates.

Cell Lines and Virus
The A673 human Ewing sarcoma cell line and Vero green monkey kidney cell line were purchased from American Type Culture Collection (Manassas, VA, USA). The TC71 human Ewing sarcoma cell line was obtained from the Children's Oncology Group repository (https://www.cccells.org). The identities of cell lines were confirmed by short tandem repeat (STR) genotyping, and mycoplasma testing was performed monthly via PCR. A673 and Vero cell lines were cultured in DMEM (Invitrogen) supplemented with 10% FBS (Invi-trogen), and TC71 was cultured in RPMI medium (Invitrogen) supplemented with 10% FBS. New stocks of cell lines were thawed every five to eight passages in vitro (approximately 1 month). The oncolytic virus rRp450, attenuated by insertion of the rat cytochrome p450 CYP2B1 gene into the viral ribonucleotide reductase ICP6 gene, was provided by E. Antonio Chiocca (Brigham and Women's Hospital, Boston, MA, USA). All virus stocks were produced and purified by the Virus Production Core at the University of Pittsburgh, School of Medicine.

Compounds and Reagents
Liposomal clodronate (Clodrosome) and control liposome were purchased from Encapsula NanoSciences (Brentwood, TN, USA). Cytokines were purchased through PeproTech (Rocky Hill, NJ, USA). Trabectedin was generously provided by Janssen Pharmaceutical Companies of Johnson and Johnson (Titusville, NJ, USA). For in vivo studies, trabectedin provided by Janssen Pharmaceutics was formulated daily at 0.0375 mg/mL in sterile purified water.

Animal Studies
All animal studies were approved by the Institutional Animal Care and Use Committee (IACUC protocol AR12-00074) for the Research Institute at Nationwide Children's Hospital. Female athymic nude mice, aged 4–6 weeks and weighing 15–25 g, were purchased from Envigo (Indianapolis, IN, USA). These mice were subcutaneously injected with 5.0×10^6 A673 or TC71 cells in a 150-μL mix of PBS and matrigel (2:1). Preformulated Clodrosome or control liposome was injected intravenously and intraperitoneally prior to rRp450 intratumoral infection for efficacy studies or Ewing sarcoma cell subcutaneous flank implantation for tumorigenesis studies as described in the figure legends. A8301 TGF-β receptor superfamily inhibitor (Sigma-Aldrich) was formulated at 5.0 mg/mL in DMSO. A8301 or equal volume of plain DMSO was diluted in PBS to 6 mg/kg A8301 and administered intraperitoneally thrice weekly as described in the figure legends. Trabectedin was formulated at 0.0375 mg/mL in the water as described above. Trabectedin or vehicle was administered intravenously by tail vein injection in a final volume of 100 μL. rRp450 was diluted in PBS to 1.0×10^8 plaque-forming units (pfu)/mL and administered intratumorally in a final volume of 100 μL. PBS was administered intratumorally as the control for rRp450 in a final volume of 100 μL.

In Vivo Efficacy Studies
When tumors reached a mean volume between 150 and 250 mm^3, mice were randomized into four study groups depending on the experiment. The specific dosing schema for each experiment is described in the figure legends. Animals were followed until the animal reached endpoint criteria (including tumor volume >2,000 mm^3, body weight loss >20%, unusual mouse behavior, lack of movement, or poor posture) or 60 days. Tumor size was measured using calipers thrice weekly, and tumor volume was calculated using the following formula: $a \times b^2 \times (\pi/6)$, where a is the length and b is the width. Mice were also weighed and observed three times per week for signs of endpoint condition. Mice that demonstrated signs of toxicity or

reached endpoint criteria were humanely euthanized by CO_2 asphyxiation and subjected to cervical dislocation as the secondary method of euthanasia.

Viral Replication

Xenograft tumors from mice treated with liposome, Clodrosome, or trabectedin regimens described in the figure legends were harvested 3, 72, and 144 hr after infection. Tumors were homogenized and subjected to three cycles of freezing and thawing before 5–8 log serial dilution in 10% FBS DMEM and inoculation of a ~90% confluent 12-well plate of Vero cells. Virus was applied for 2 hr before adding overlay media (1% carboxymethylcellulose [CMC], 1× MEM, 10% FBS) and incubating in a 37°C incubator for 2 days. Plates were stained in crystal violet for 20 min, washed in tap water, and dried overnight. Viral plaques are counted and multiplied by serial dilution to determine viral titer. Each graph is the accumulation of two to three experimental replicates.

Flow Cytometry

Splenocytes or single tumor cell suspensions were prepared as described previously.[50] 1×10^6 cells were blocked with 5% mouse Fc blocking reagent (2.4G2; BD Biosciences) in fluorescence-activated cell sorting (FACS) buffer (1% FBS and 1 mM EDTA in PBS) and stained with antibodies against CD206-fluorescein isothiocyanate (FITC) (C068C2), CD49b-PE (DX5), Ly6C-antigen-presenting cell (APC) (AL-21), CD11c-PerCP/Cy5.5 (N418), CD11b-Violet 421 (M1/70), F4/80-PE-Cy7 (BM8), and Ly-6G-APC-Cy7 (1A8) on ice for 30 min. Stained cells were washed with FACS buffer and fixed in 0.5% paraformaldehyde. Samples were acquired on a BD FACS LSR II (BD Biosciences), and cell infiltrate analysis was carried out using the FlowJo software, version 10.0.3 (Tree Star). All the staining antibodies were obtained from BioLegend except for anti-Ly6C (BD Biosciences).

Coculture Cytotoxicity

Bone marrow-derived macrophages (BMDMs) were positively selected from athymic nude mouse bone marrow using F4/80+ antibodies conjugated to magnetic beads, then incubated in 20% FBS RPMI supplemented with 200 ng/mL macrophage-colony stimulating factor (M-CSF) for >5 days. BMDMs were then left unstimulated in 20% FBS RPMI or supplemented with 20 ng/mL IFNγ, 20 ng/mL IFNγ + 5 ng/mL LPS, 5 ng/mL LPS, 20 ng/mL IL-4, 20 ng/mL IL-10, or 20 ng/mL TGF-β for 48 hr. Two thousand A673 or TC71 Ewing sarcoma cells were plated in 96-well plates alone or directly cocultured with 200 cells/mL BMDM cultures in 10% FBS DMEM stimulated with the respective cytokines of the BMDMs for 2 hr. Cocultures were then infected with oHSVrRp450 at MOI 0.1 or 0 and incubated at 37°C for 6 days with additional cytokine stimulation to starting concentrations every 48 hr. Cell viability was determined using the CellTiter 96 (Promega) MTS (3-(4,5-dimethylthiazol-2-yl)-5-(3-carboxymethoxyphenyl)-2-(4-sulfophenyl)-2H-tetrazolium) assay kit. Cell viability was calculated by recording the 490 nm absorbance values and omitting the values of the infected BMDM cultures alone from their respective Ewing sarcoma cell cocultures. The Ewing sarcoma absorbance values where then normalized to the values of the uninfected Ewing sarcoma alone-treated wells.

Biomark qPCR Array

Whole tumor lysates from Clodrosome/Liposome PBS/rRp450-treated A673 xenografts described above were harvested at 3 hr, 5 days, and 25 days postinfection. F4/80+ tumor macrophages lysates were harvested from Clodrosome/Liposome PBS/rRp450-treated A673 xenografts described above using a 44%/66% percoll RPMI gradient extraction of the buffy coat, followed by positive selection of F4/80+ tumor macrophages using antibody-conjugated magnetic beads. The stimulated BMDMs cultured alone and cocultured with Ewing sarcoma cells described above were harvested and lysed. With the assistance of the Ohio State University Genomics Core, RNA was extracted from these samples using an RNeasy Plus Mini Kit (Qiagen), diluted to a concentration of 10 ng/μL, and run on a Biomark HD qPCR array chip (Fluidigm) with a custom panel of gene primers designed by Fluidigm targeting genes we selected including housekeeping, HSV-1, and genes known to be differentially expressed in variously polarized macrophages. See the Delta Gene Assay Report in the Supplemental Information for a complete listing of genes tested and their amplicon sizes. Relative RNA expression values for each gene were normalized to actin expression for each treatment condition using the $2^{-\Delta\Delta Ct}$ method. See Tables S1, S2, and S3 for raw threshold cycle (Ct) data and normalization calculations for all of the genes tested.

Statistical Analysis

Survival studies were analyzed using Mantel-Cox log rank test. Comparison of samples with normal distribution was analyzed using Student's t test. Difference among group means was determined with ANOVA. Statistical tests were run on Microsoft Excel or GraphPad Prism v7.0. Significant differences in samples groups were determined by $p < 0.05$, whereas significant trends were determined by $0.05 < p < 0.15$.

SUPPLEMENTAL INFORMATION

Supplemental Information includes two figures, one Delta Gene Assay Report, and three tables, and can be found with this article online at https://doi.org/10.1016/j.omto.2018.10.001.

CONFLICTS OF INTEREST

None of the authors have any disclosures or conflicts of interest.

ACKNOWLEDGMENTS

REFERENCES

1. Fujiwara, T., Fukushi, J., Yamamoto, S., Matsumoto, Y., Setsu, N., Oda, Y., Yamada, H., Okada, S., Watari, K., Ono, M., et al. (2011). Macrophage infiltration predicts a poor prognosis for human Ewing sarcoma. Am. J. Pathol. 179, 1157–1170.

2. May, W.A., Lessnick, S.L., Braun, B.S., Klemsz, M., Lewis, B.C., Lunsford, L.B., Hromas, R., and Denny, C.T. (1993). The Ewing's sarcoma EWS/FLI-1 fusion gene encodes a more potent transcriptional activator and is a more powerful transforming gene than FLI-1. Mol. Cell. Biol. 13, 7393–7398.

3. Theisen, E.R., Pishas, K.I., Saund, R.S., and Lessnick, S.L. (2016). Therapeutic opportunities in Ewing sarcoma: EWS-FLI inhibition via LSD1 targeting. Oncotarget 7, 17616–17630.

4. May, W.A., Gishizky, M.L., Lessnick, S.L., Lunsford, L.B., Lewis, B.C., Delattre, O., Zucman, J., Thomas, G., and Denny, C.T. (1993). Ewing sarcoma 11;22 translocation produces a chimeric transcription factor that requires the DNA-binding domain encoded by FLI1 for transformation. Proc. Natl. Acad. Sci. USA 90, 5752–5756.

5. Denton, N.L., Chen, C.-Y., Scott, T.R., and Cripe, T.P. (2016). Tumor-associated macrophages in oncolytic virotherapy: friend or foe? Biomedicines 4, E13.

6. Teicher, B.A., Bagley, R.G., Rouleau, C., Kruger, A., Ren, Y., and Kurtzberg, L. (2011). Characteristics of human Ewing/PNET sarcoma models. Ann. Saudi Med. 31, 174–182.

7. Varghese, S., and Rabkin, S.D. (2002). Oncolytic herpes simplex virus vectors for cancer virotherapy. Cancer Gene Ther. 9, 967–978.

8. Gujar, S., Dielschneider, R., Clements, D., Helson, E., Shmulevitz, M., Marcato, P., Pan, D., Pan, L.Z., Ahn, D.G., Alawadhi, A., and Lee, P.W. (2013). Multifaceted therapeutic targeting of ovarian peritoneal carcinomatosis through virus-induced immunomodulation. Mol. Ther. 21, 338–347.

9. Cripe, T.P., Chen, C.Y., Denton, N.L., Haworth, K.B., Hutzen, B., Leddon, J.L., Streby, K.A., Wang, P.Y., Markert, J.M., Waters, A.M., et al. (2015). Pediatric cancer gone viral. Part I: strategies for utilizing oncolytic herpes simplex virus-1 in children. Mol. Ther. Oncolytics 2, 15015.

10. Friedman, G.K., Beierle, E.A., Gillespie, G.Y., Markert, J.M., Waters, A.M., Chen, C.Y., Denton, N.L., Haworth, K.B., Hutzen, B., Leddon, J.L., et al. (2015). Pediatric cancer gone viral. Part II: potential clinical application of oncolytic herpes simplex virus-1 in children. Mol. Ther. Oncolytics 2, 15016.

11. Andtbacka, R.H., Ross, M., Puzanov, I., Milhem, M., Collichio, F., Delman, K.A., Amatruda, T., Zager, J.S., Cranmer, L., Hsueh, E., et al. (2016). Patterns of clinical response with talimogene laherparepvec (T-VEC) in patients with melanoma treated in the OPTiM phase III clinical trial. Ann. Surg. Oncol 23, 4169–4177.

12. Zheng, Y.H., Deng, Y.Y., Lai, W., Zheng, S.Y., Bian, H.N., Liu, Z.A., Huang, Z.F., Sun, C.W., Li, H.H., Luo, H.M., et al. (2018). Effect of bone marrow mesenchymal stem cells on the polarization of macrophages. Mol. Med. Rep. 17, 4449–4459.

13. Chen, C.H., Chen, W.Y., Lin, S.F., and Wong, R.J. (2014). Epithelial-mesenchymal transition enhances response to oncolytic herpesviral therapy through nectin-1. Hum. Gene Ther. 25, 539–551.

14. Meisen, W.H., Wohleb, E.S., Jaime-Ramirez, A.C., Bolyard, C., Yoo, J.Y., Russell, L., Hardcastle, J., Dubin, S., Muili, K., Yu, J., et al. (2015). The impact of macrophage- and microglia-secreted TNFα on oncolytic HSV-1 therapy in the glioblastoma tumor microenvironment. Clin. Cancer Res. 21, 3274–3285.

15. Liu, H., Yuan, S.J., Chen, Y.T., Xie, Y.B., Cui, L., Yang, W.Z., Yang, D.X., and Tian, Y.T. (2013). Preclinical evaluation of herpes simplex virus armed with granulocyte-macrophage colony-stimulating factor in pancreatic carcinoma. World J. Gastroenterol. 19, 5138–5143.

16. Francis, L., Guo, Z.S., Liu, Z., Ravindranathan, R., Urban, J.A., Sathaiah, M., Magge, D., Kalinski, P., and Bartlett, D.L. (2016). Modulation of chemokines in the tumor microenvironment enhances oncolytic virotherapy for colorectal cancer. Oncotarget 7, 22174–22185.

17. Ugel, S., De Sanctis, F., Mandruzzato, S., and Bronte, V. (2015). Tumor-induced myeloid deviation: when myeloid-derived suppressor cells meet tumor-associated macrophages. J. Clin. Invest. 125, 3365–3376.

18. Wang, N., Liang, H., and Zen, K. (2014). Molecular mechanisms that influence the macrophage m1-m2 polarization balance. Front. Immunol. 5, 614.

19. Kim, C.C., Nakamura, M.C., and Hsieh, C.L. (2016). Brain trauma elicits non-canonical macrophage activation states. J. Neuroinflammation 13, 117.

20. Iwata, H., Goettsch, C., Sharma, A., Ricchiuto, P., Goh, W.W., Halu, A., Yamada, I., Yoshida, H., Hara, T., Wei, M., et al. (2016). PARP9 and PARP14 cross-regulate macrophage activation via STAT1 ADP-ribosylation. Nat. Commun. 7, 12849.

21. Murray, P.J., Allen, J.E., Biswas, S.K., Fisher, E.A., Gilroy, D.W., Goerdt, S., Gordon, S., Hamilton, J.A., Ivashkiv, L.B., Lawrence, T., et al. (2014). Macrophage activation and polarization: nomenclature and experimental guidelines. Immunity 41, 14–20.

22. Currier, M.A., Eshun, F.K., Sholl, A., Chernoguz, A., Crawford, K., Divanovic, S., Boon, L., Goins, W.F., Frischer, J.S., Collins, M.H., et al. (2013). VEGF blockade enables oncolytic cancer virotherapy in part by modulating intratumoral myeloid cells. Mol. Ther. 21, 1014–1023.

23. Currier, M.A., Gillespie, R.A., Sawtell, N.M., Mahller, Y.Y., Stroup, G., Collins, M.H., Kambara, H., Chiocca, E.A., and Cripe, T.P. (2008). Efficacy and safety of the oncolytic herpes simplex virus rRp450 alone and combined with cyclophosphamide. Mol. Ther. 16, 879–885.

24. Aghi, M., Chou, T.C., Suling, K., Breakefield, X.O., and Chiocca, E.A. (1999). Multimodal cancer treatment mediated by a replicating oncolytic virus that delivers the oxazaphosphorine/rat cytochrome P450 2B1 and ganciclovir/herpes simplex virus thymidine kinase gene therapies. Cancer Res. 59, 3861–3865.

25. Bolyard, C., Meisen, W.H., Banasavadi-Siddegowda, Y., Hardcastle, J., Yoo, J.Y., Wohleb, E.S., Wojton, J., Yu, J.G., Dubin, S., Khosla, M., et al. (2017). BAI1 orchestrates macrophage inflammatory response to HSV infection—implications for oncolytic viral therapy. Clin. Cancer Res. 23, 1809–1819.

26. Hutzen, B., Chen, C.Y., Wang, P.Y., Sprague, L., Swain, H.M., Love, J., Conner, J., Boon, L., and Cripe, T.P. (2017). TGF-β inhibition improves oncolytic herpes viroimmunotherapy in murine models of rhabdomyosarcoma. Mol. Ther. Oncolytics 7, 17–26.

27. Germano, G., Frapolli, R., Belgiovine, C., Anselmo, A., Pesce, S., Liguori, M., Erba, E., Uboldi, S., Zucchetti, M., Pasqualini, F., et al. (2013). Role of macrophage targeting in the antitumor activity of trabectedin. Cancer Cell 23, 249–262.

28. Nakai, T., Imura, Y., Tamiya, H., Yamada, S., Nakai, S., Yasuda, N., Kaneko, K., Outani, H., Takenaka, S., Hamada, K., et al. (2017). Trabectedin is a promising antitumor agent potentially inducing melanocytic differentiation for clear cell sarcoma. Cancer Med. 6, 2121–2130.

29. Herzog, J., von Klot-Heydenfeldt, F., Jabar, S., Ranft, A., Rossig, C., Dirksen, U., Van den Brande, J., D'Incalci, M., von Luettichau, I., Grohar, P.J., et al. (2016). Trabectedin followed by irinotecan can stabilize disease in advanced translocation-positive sarcomas with acceptable toxicity. Sarcoma 2016, 7461783.

30. Hernando-Cubero, J., Sanz-Moncasi, P., Hernández-García, A., Pajares-Bernard, I., and Martínez-Trufero, J. (2016). Metastatic extraskeletal Ewing's sarcoma treated with trabectedin: a case report. Oncol. Lett. 12, 2936–2941.

31. Grohar, P.J., Segars, L.E., Yeung, C., Pommier, Y., D'Incalci, M., Mendoza, A., and Helman, L.J. (2014). Dual targeting of EWS-FLI1 activity and the associated DNA damage response with trabectedin and SN38 synergistically inhibits Ewing sarcoma cell growth. Clin. Cancer Res. 20, 1190–1203.

32. Wang, Y.C., He, F., Feng, F., Liu, X.W., Dong, G.Y., Qin, H.Y., Hu, X.B., Zheng, M.H., Liang, L., Feng, L., et al. (2010). Notch signaling determines the M1 versus M2 polarization of macrophages in antitumor immune responses. Cancer Res. 70, 4840–4849.

33. Saha, D., Martuza, R.L., and Rabkin, S.D. (2017). Macrophage polarization contributes to glioblastoma eradication by combination immunovirotherapy and immune checkpoint blockade. Cancer Cell 32, 253–267.e5.

34. Delwar, Z.M., Kuo, Y., Wen, Y.H., Rennie, P.S., and Jia, W. (2018). Oncolytic virotherapy blockade by microglia and macrophages requires STAT1/3. Cancer Res. 78, 718–730.

35. Borgoni, S., Iannello, A., Cutrupi, S., Allavena, P., D'Incalci, M., Novelli, F., and Cappello, P. (2017). Depletion of tumor-associated macrophages switches the epigenetic profile of pancreatic cancer infiltrating T cells and restores their anti-tumor phenotype. OncoImmunology 7, e1393596.

36. Igarashi, K., Murakami, T., Kawaguchi, K., Kiyuna, T., Miyake, K., Zhang, Y., Nelson, S.D., Dry, S.M., Li, Y., Yanagawa, J., et al. (2017). A patient-derived orthotopic xenograft (PDOX) mouse model of a cisplatinum-resistant osteosarcoma lung metastasis that was sensitive to temozolomide and trabectedin: implications for precision oncology. Oncotarget 8, 62111–62119.

37. Sica, A., and Massarotti, M. (2017). Myeloid suppressor cells in cancer and autoimmunity. J. Autoimmun. 85, 117–125.

38. Elliott, L.A., Doherty, G.A., Sheahan, K., and Ryan, E.J. (2017). Human tumor-infiltrating myeloid cells: phenotypic and functional diversity. Front. Immunol. 8, 86.

39. Kumar, V., Patel, S., Tcyganov, E., and Gabrilovich, D.I. (2016). The nature of myeloid-derived suppressor cells in the tumor microenvironment. Trends Immunol. 37, 208–220.

40. Gordon, D.J., Motwani, M., and Pellman, D. (2016). Modeling the initiation of Ewing sarcoma tumorigenesis in differentiating human embryonic stem cells. Oncogene 35, 3092–3102.

41. Ferrari, A., Dirksen, U., and Bielack, S. (2016). Sarcomas of soft tissue and bone. Prog. Tumor Res. 43, 128–141.

42. Chen, D., Xie, J., Fiskesund, R., Dong, W., Liang, X., Lv, J., Jin, X., Liu, J., Mo, S., Zhang, T., et al. (2018). Chloroquine modulates antitumor immune response by resetting tumor-associated macrophages toward M1 phenotype. Nat. Commun. 9, 873.

43. Singh, M.K., Jamal, F., Dubey, A.K., Shivam, P., Kumari, S., Pushpanjali, Ahmed, G., Dikhit, M.R., Narayan, S., Das, V.N.R., et al. (2018). Co-factor-independent phosphoglycerate mutase of Leishmania donovani modulates macrophage signalling and promotes T-cell repertoires bearing epitopes for both MHC-I and MHC-II. Parasitology 145, 292–306.

44. Turaj, A.H., Hussain, K., Cox, K.L., Rose-Zerilli, M.J.J., Testa, J., Dahal, L.N., Chan, H.T.C., James, S., Field, V.L., Carter, M.J., et al. (2017). Antibody tumor targeting is enhanced by CD27 agonists through myeloid recruitment. Cancer Cell 32, 777–791.e6.

45. Ratti, C., Botti, L., Cancila, V., Galvan, S., Torselli, I., Garofalo, C., Manara, M.C., Bongiovanni, L., Valenti, C.F., Burocchi, A., et al. (2017). Trabectedin overrides osteosarcoma differentiative block and reprograms the tumor immune environment enabling effective combination with immune checkpoint inhibitors. Clin. Cancer Res. 23, 5149–5161.

46. Leddon, J.L., Chen, C.Y., Currier, M.A., Wang, P.Y., Jung, F.A., Denton, N.L., Cripe, K.M., Haworth, K.B., Arnold, M.A., Gross, A.C., et al. (2015). Oncolytic HSV virotherapy in murine sarcomas differentially triggers an antitumor T-cell response in the absence of virus permissivity. Mol. Ther. Oncolytics 1, 14010.

47. Bartee, E., and Li, Z. (2017). In vivo and in situ programming of tumor immunity by combining oncolytics and PD-1 immune checkpoint blockade. Exp. Hematol. Oncol. 6, 15.

48. Rojas, J.J., Sampath, P., Hou, W., and Thorne, S.H. (2015). Defining effective combinations of immune checkpoint blockade and oncolytic virotherapy. Clin. Cancer Res. 21, 5543–5551.

49. Guo, Z., Wang, H., Meng, F., Li, J., and Zhang, S. (2015). Combined Trabectedin and anti-PD1 antibody produces a synergistic antitumor effect in a murine model of ovarian cancer. J. Transl. Med. 13, 247.

50. Chen, C.Y., Wang, P.Y., Hutzen, B., Sprague, L., Swain, H.M., Love, J.K., Stanek, J.R., Boon, L., Conner, J., and Cripe, T.P. (2017). Cooperation of oncolytic herpes virotherapy and PD-1 blockade in murine rhabdomyosarcoma models. Sci. Rep. 7, 2396.